

Investigation of characteristics of Silicon APDs for use in scintillating fiber trackers

J.Bähr, H.Bärwolff*, V.Kantserov†

22/01/99

1 Introduction

Scintillating fiber detectors for tracking and triggering are widely used in experiments of particle physics, because of numerous advantages, so in UA2 [1], in the CHORUS experiment [2], in the D0 upgrade detector [3], in the Forward Proton Spectrometer FPS of H1 at HERA [4]. In 1997 a fiber detector was developed as second solution for an inner tracker detector of the HERA-B experiment [5]. It is also discussed to use fiber detectors for tracking and triggering, for example for an experiment at a future Electron-Positron-Collider [6]. The investigations described below are just motivated by the necessity to find new optimized readout solutions for scintillating fibers.

Different principles are used for the optoelectronic readout up to now, e.g. combination of Image Intensifiers (II) with CCDs, Visible Light Photon Counters (VLPCs) and multichannel photomultipliers (PSPMs). These types of devices have different advantages and drawbacks. One of the most limiting factors of PM solutions is the relative low quantum efficiency (QE) of photocathodes. There is a possibility to overcome this limitation by use of semiconducting devices. That is the reason for the investigation of Avalanche Photodiodes (APDs), which have also a certain internal gain.

One can observe a steadily ongoing development of APDs for applications in detectors of particle physics in the last years [7]. This is the base for tests of different APDs - commercially available devices and prototypes - for applications in scintillating fiber triggers and trackers described below. Optoelectronic devices are characterized by a couple of basic parameters: QE, collecting or internal efficiency, gain, noise, signal-to-noise-ratio, time behaviour (pulse response, dead time) and so on. To overcome the problem of QE using a "new" detector principle, one has to guarantee, that all other parameters of the new device will not be essentially worse as the standard solutions, for example the use of PMs. Most of the parameters mentioned above were measured for a sample of different prototypes as outlined in the next chapters. APDs according to their characteristic curve of operation can be operated in two basic modes: in

*Fachhochschule Köln, Fachbereich Elektrotechnik

†On leave from Moscow Experimental Physics Institute

the avalanche mode having a medium gain and in the Geiger mode with an operating voltage greater as the breakthrough voltage. The investigation described in this paper concern exclusively the operation in the avalanche mode.

2 APD samples and producer data

Avalanche photodiodes (APDs) from Hamamatsu¹ and test samples of APDs with MRS (metall-resistive layer semiconductors) structure [8] from Dubna were used for testing. Basic characteristics from the data sheet are given in table 1.

Parameter	Symbol	S5443	S2384	MRS	HPR
Peak Sensitiv. Wavelength/nm	λ_p	620	800	-	
Quantum efficiency	η	65%@500 nm	50%@540 nm	55%@480 nm	
Dark current/nA (typical)	I_d	1.0	1.0	≤ 1	≤ 1
Dark current/nA (maximum)	I_d	10.0	10.0	≤ 1	≤ 1
Breakdown Voltage/V	U_{BR}	150	80÷100	30÷40	324
Temp.Coeff. of $U_{BR}/(V/grd)$		0.14	0.65		
Cut-off Frequency/MHz	f_c	250	120		
Terminal Capacity/pF	C_t	15	40	40	
Excess Noise Index	X	0.28	0.3		
Gain	M	50	60	10^4	
Active area/mm	Φ	1	3	0.5×0.5	

Table 1: Basic characteristics of investigated APDs according to data sheets. HPR means a prototype of recently developed APDs from Hamamatsu.

3 Dark current measurements

One of the most important parameters to be considered when selecting on APD is the dark current. A small dark current makes an APD suitable for operation below the breakthrough voltage U_{BR} or of single photon counting above U_{BR} . Cooling can reduce the dark current since the dependence of the dark current on temperature is exponential. We have measured the dark current as a function of the voltage of all APDs listed in table 1. The dependence of the dark current on the voltage is shown in fig. 1. Below the breakthrough voltage the dark current is essentially less than 1 nA for all devices. Above the breakthrough voltage the gain rises rapidly due to the transition from avalanche to Geiger mode.

¹Hamamatsu Photonics K.K., Electron tube division, 314-5, Shimokanzo, Tokoyoka village. Iwata-gun, Shizuoka-ken, Japan

4 Efficiency measurements using LEDs

Light emitting diodes (LEDs) were used for the imitation of scintillating light in the first steps of investigations. The procedure of the calibration of the amount of light emitted by the LEDs is described in the next section.

4.1 Calibration

The current and the corresponding brightness of the LEDs are determined by the LED driver. The pulse duration of the LED current is set to about 20 ns, the amplitude can be adjusted. The blue LED is emitting in the spectral region of about $455\div 495$ nm , the green LED in the region of $495\div 575$ nm.

The spectral sensitivity of APDs investigated and of the photomultiplier (PM) XP 2020 from Philips², which was used for calibration is shown in fig. 2. The light output of the LED was reduced to see the one-photoelectron peak of the PM, as shown in fig. 3. The mean value and the variance are determined by a Gauss-fit, the pedestal was subtracted. Using this data and the spectral sensitivity of LED and PM, the number of incident photons can be estimated.

The calibration of the LEDs was performed using a PM XP2020. In fig. 4 the number of photoelectrons detected by the PM XP2020 in dependence on the LED current (brightness) is shown for the blue and green LED. Using the spectral characteristics of the XP2020 (fig.2b), one can calculate the number of photoelectrons depending on the LED current, whereby the error of the estimation of photoelectrons amounts to about 50 %. This is an upper limit of the estimation of the error, which is basing on contributions of uncertainties of the optical contact between LED, fiber and PM, on a certain error of the quantum efficiency of the individual PM and finally on the error of the measurement of the amplitude spectra of the PM signal.

4.2 Preamplifier

In all measurements with APD a current amplifier of Radeka [9] is used for the amplification of the signal and the optimization of the electrical matching of the detector output to the front-end electronics. The characteristics of the preamplifier are listed in table 2.

4.3 Setup

The scheme of the experimental setup for the investigation of the APD sensitivity in the avalanche mode using LEDs is shown in fig.5. The pulse length of the output signals of both discriminators is equal and amounts to 50 ns.

²Philips Photonique , Av. Roger Roacier, B.P.520, 19106 Brive, France

The MRS APD is mounted on a Peltier-element and can be investigated at lower temperatures. The cooling below $+10^{\circ}\text{C}$ resulted in some problems created by the luminosity of condensed water on the APD surface leading to surface discharges.

The preamplifier is mounted in minimum distance to the detector in order to minimize the overall capacity of the setup. The following elements of the setup are standard NIM modules.

Input resistance	R_{in} 50 Ohms
Gain	10^4 V/A at 10 kOhms
Noise	2000e
R_{out}	50 Ohms (differential)
Rise time	$\tau_{rise} = 8$ ns
Power supply	± 12 V

Table 2: Characteristics of the preamplifier

LED	APD	Amplifier	U/V	Thrshld./mV
green	S2384	Radeka	-89	27.5
green	S5343	Rad.+Lecroy	-147	30
green	HPR	Rad.+Lecroy	-324	30
green	MRS N.2(+20°C)	Radeka	-49.1	40
green	MRS N.2(+10°C)	Radeka	-48.6	40
blue	S5343	Radeka	-148	30
blue	HPR	Rad.+Lecroy	-324	40
blue	MRS N.2(+20°C)	Radeka	-49.0	40
blue	MRS N.2(+10°C)	Radeka	-48.7	40

Table 3: Parameters of efficiency measurements

4.4 Results

The criterion for the estimation of the APD sensitivity is the efficiency of the detection of a light signal in correlation to the signal of the pulse generator of the LED (fig. 5).

In figure 6 the efficiency of different APDs excited in the blue or green spectral region is shown. In table 3 parameters of the measurements are given. The results of the efficiency measurement of different APDs with LEDs are given in table 4. The best results were achieved with both MRS diodes at a temperature of 10°C , whereby the noise is of the order of 500 kHz. The sensitivity of 20 photons corresponds to a signal

of 4 photoelectrons of a PM with a QE of 20 %.

The efficiency of the APDs can also be measured comparing the amplitude spectrum of the APD illuminated by LED light. In fig.7 the pedestal and the amplitude spectrum of a Hamamatsu APD type S5343 excited with light pulses of 100 photons is shown. The upper part of the figure shows the pedestal, the corresponding amplitude spectrum is shown in the lower part of the figure. A clear separation of the two regions is observed.

Avalanche mode					
APD	Temperat.	Green		Blue	
		N_{ph} at 95%Eff.	Noise cnts./s	N_{ph} at 95%Eff.	Noise cnts./s
S2384	+20°C	150	270*10 ³	1000	200*10 ³
S5343	+20°C	40	40*10 ³	160	900*10 ³
MRS No.1(38)	+20°C	90	700*10 ³	90	130*10 ³
MRS No.1(38)	+10°C	70	600*10 ³	25	600*10 ³
MRS No.2(48)	+20°C	90	200*10 ³	100	30*10 ³
MRS No.2(48)	+10°C	50	300*10 ³	20	500*10 ³
HPR	+20°C	45	270*10 ³	40	200*10 ³

Table 4: Sensitivity characteristics of measured APDs (N_{ph} : Number of photons)

5 Double pulse resolution

To estimate the time resolution of APDs , the efficiency of the detection of double light pulses with a time difference of 100 ns between both pulses is measured, which is given by the length of the two single pulses of 50 ns at the output of the discriminators. The results are shown in fig. 8 and table 5. For the given conditions the efficiency of the registration of double pulses is equal to the efficiency of the registration of single pulses for all tested APDs. That means, that the time resolution is no limiting factor for pulse sequences of 100 ns.

6 Measurements using scintillating fibers

The experimental results of the efficiency measurements of different APDs using LEDs show, that the most promising samples are the MRS APDs and the Hamamatsu prototypes (HPR). The MRS samples gave the best results at lower temperatures (in our case up to 10°C). Both types of APDs have a blue-shifted spectral sensitivity which matches to the emission spectra of usual blue scintillators. To get more precise data of the number of photons coming from the light source we used scintillating fibers to excite the APD samples. In the experiments those APD samples were used, which

LED	APD	Pulse	Amplifier	U/V	Thrshld./mV	Noise/Hz
green	S5343	double	Rad.+Lecroy	-147	40	15*10 ³
green	S5343	single	Rad.+Lecroy	-147	40	15*10 ³
green	MRS N.2	double	Radeka	-49.3	30	180*10 ³
green	MRS N.2	single	Radeka	-49.3	30	180*10 ³
blue	S5343	double	Rad.+Lecroy	-147	30	30*10 ³
blue	S5343	single	Rad.+Lecroy	-147	30	30*10 ³
blue	MRS N.2	double	Radeka	-49.0	40	30*10 ³
blue	MRS N.2	single	Radeka	-49.0	40	30*10 ³

Table 5: Double pulse characteristics: Parameters and results

gave the best results excited by blue emitting LEDs, i.e. MRS APDs and Hamamatsu Prototypes (HPR).

6.1 Experimental setup

The experimental setup for the use of scintillation light is shown in fig. 9. The scintillator plate and the scintillating fiber are excited by a radioactive ¹⁰⁶Ru source using a collimator with a slit of 0.5 mm. The coincidence of the signals of the PMs No.2, 3, 4 results in a trigger signal. The signal of the APD sample is detected in coincidence with the trigger signal. Efficiency is the ratio of counts of the APD in coincidence with trigger divided by the number of trigger counts.

6.2 Results

The Hamamatsu prototype (HPR) APD gives a weak response to the scintillator light working without cooling and using the Radeka type preamplifier. In this case the bias voltage was -325 V, i.e. 1 V higher than the breakthrough voltage. In this mode a high noise level is found and it will be difficult to use such signals. It might be possible, that cooling of the prototype APD would result in an essential higher efficiency. The MRS APDs show essential better results, especially MRS No.2. The signals of this APD measured using the oscilloscope in the average and sampling mode are shown in fig. 10. It is seen, that MRS No.2 gives really acceptable signals in the cooling regime down to 10° Celsius. The detection efficiency of scintillating fiber signals (KURARAY³ SCSF 78, 0.5 mm fiber diameter) of APD MRS No.2 is given in table 6.

³KURARAY Co. LTD., Nikonbashi, Chuo-ku, Tokyo 103, Japan

Temperatur	Efficiency
+20°C	0.63
+10°C	0.72

Table 6: Efficiency of the registration of scintillating light from blue fibers from KURARAY SCSF 78 (0.5 mm) by MRS No.2

Device	Voltage/V	Temperat.	KUR.SCSF 0.5 mm diam.		pol.hi.tech. 1.0 mm diam.	
			U_{signal}	Noise	U_{Signal}	Noise
HPR No.14	-326	+20°	1.5 mV	5 MHz	2.0 mV	5 MHz
MRS No.1	-39.0	+20°	2.0 mV	5 MHz	1.0 mV	5 MHz
MRS No.1	-39.0	+10°	15.0 mV	1.0 MHz	-	-
MRS No.2		+20°	10.0 mV	0.5 MHz	10.0 mV	0.6 MHz
MRS No.2		+10°	70.0 mV	0.3 MHz	-	-

Table 7: Results of the detection of scintillating light from fibers KURARAY SCSF 78 0.5 mm and pol.hi.tech. (420 nm) 1.0 mm diameter

The results of the detection of scintillator light from fibers of 0.5 mm (KURARAY SCSF78) and 1 mm diameter (pol.hi.tech.⁴ 420 nm) are given in table 7.

The results of measurements using fibers of different producers and the MRS APD No.2(48) are shown in table 8.

No correction was made to compensate the geometrical coupling losses of the fiber of 1 mm diameter to the MRS APD of 0.5 mm diameter. One can estimate losses of factor 4 in amplitude.

The figures of table 6 can be compared with a direct measurement of a KURARAY fiber of 0.5 mm diameter using a PM XP2020 resulting in an efficiency of 58%.

7 Summary

The results of the investigations of APDs to registrate scintillation light from fibers in the avalanche mode show the principal feasibility of this method. Cooling and the application of adequate electronics which is optimized for APDs should allow to increase the efficiency of the registration of scintillation light.

⁴pol.hi.tech., s.r.l., S.P. Turanense, 67061 Carsoli(AQ), Italy

Type of fibers	Fiber diameter	$U_{Signal}(APD)$	$U_{Signal}(XP2020)$ (arb.units)	Eff.
KURARAY SCSF 78	0.5 mm	16 mV	362	63%
pol.hi.tech. 460 nm	0.5 mm	14 mV	353	50%
KURARAY 3HF	0.5 mm	4 mV	329	-
pol.hi.tech. 480 nm	0.5 mm	3 mV	337	-
Bicron BCF-60	0.5 mm	5 mV	329	-
pol.hi.tech. 420 nm	1.0 mm	12 mV	350	42%

Table 8: Results of the detection of scintillating light from fibers of different producers using the MRS APD No.2(48) at 20⁰C and PM XP2020 at 2300 V as reference

8 Acknowledgement

We thank Zair Sadygov from Dubna for providing us with the interesting MRS prototypes. We acknowledge the benefit from many fruitful discussions with R.Nahnauer and R.Leiste.

References

- [1] Ansorge, R., et al., NIM A265, 33(1988)
- [2] Annies, P., et al., NIM A367, 367(1995)
- [3] Bross, A.D., Nucl. Phys. B (Proc.Suppl.) 44, 12 (1995)
Adams D., et al., Nucl.Phys. B (Proc.Suppl.) 44, 332 (1995)
- [4] Bähr, J., et al., Proceedings of the 28th Intern. Conf. on High Energy Physics, Warsaw, Poland, 1996, eds. Z.Ajduk, A.K.Wroblewski V.II, p.1759
- [5] Aschenauer, E.C. et al., DESY-Preprint 98-074, 1998
- [6] Leich, H., DESY-Preprint 98-002, 1998
- [7] Farrell, R. et al., NIM A387 (1997) 194
Elias, J.E., NIM A387 (1997) 104
Bacchetta, N. et al., NIM A387 (1997) 225
Okumara, S. et al., NIM A388 (1997) 235
Kirn, Th. et al., NIM A387 (1997) 199
Nonaka, N. et al., NIM A383 (1996) 81
Brückner, W. et al., CERN/PPE 91-146
Deiters, K. et al., NIM A387 (1997) 211
Tapan, I. et al., NIM A388 (1997) 79
Farrell, R. et al., NIM A353 (1994) 176

Sadygov, Z.Y. et al., IEEE, Trans. Nucl.Sci., 43 (1996) 1009
Carrier, C. and R.Lecomte,IEEE Trans. on Nucl. Sci.. 37, 2, (1990), 209
Karar et al., X-LPNHE/95-10, 1995
Si Mohand, D. et al., LYCEN 9613, CMS TN/96-052 1996
Jeanney, C. et al., DPhPE 91-15, Saclay, 1991

[8] Antich, P.P. et al., NIM A389(1997) 491

[9] Radeka, V. et al., NIM A242(1985) 75

[10] Philips Data Handbook Photomultiplier PC04, (1990), The Netherlands

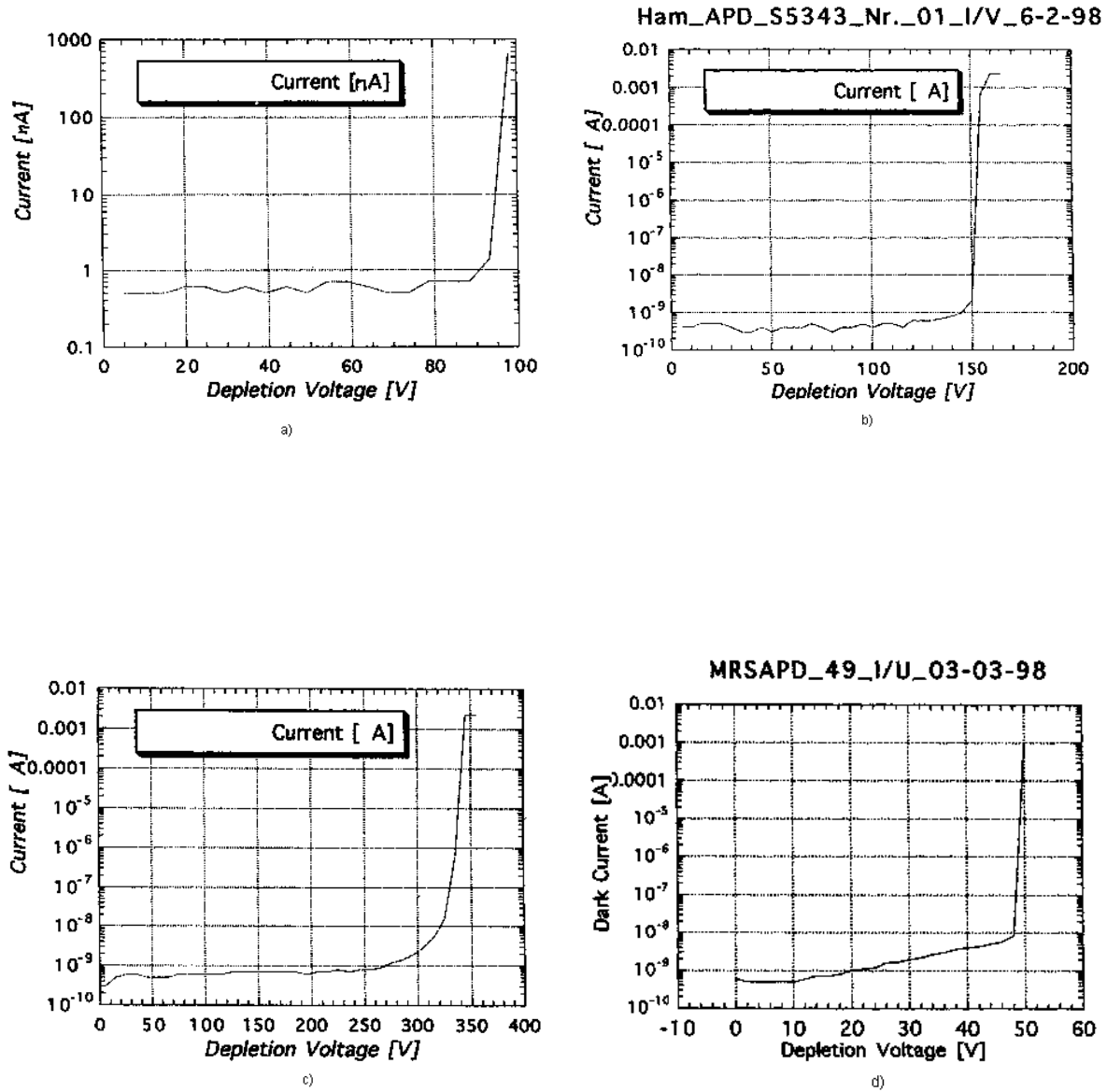


Figure 1: Dependence of dark current on bias voltage of different APDs a) S2384, b) S5343, c) HPR, d) MRS No.2

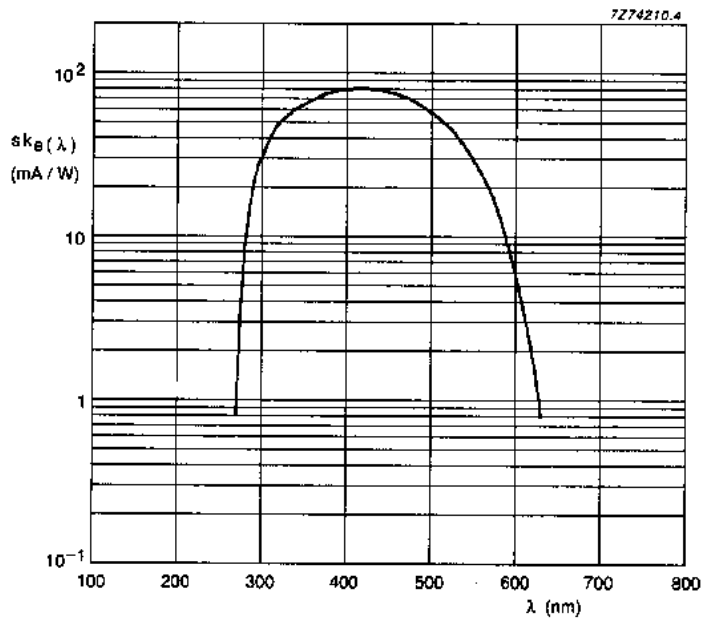
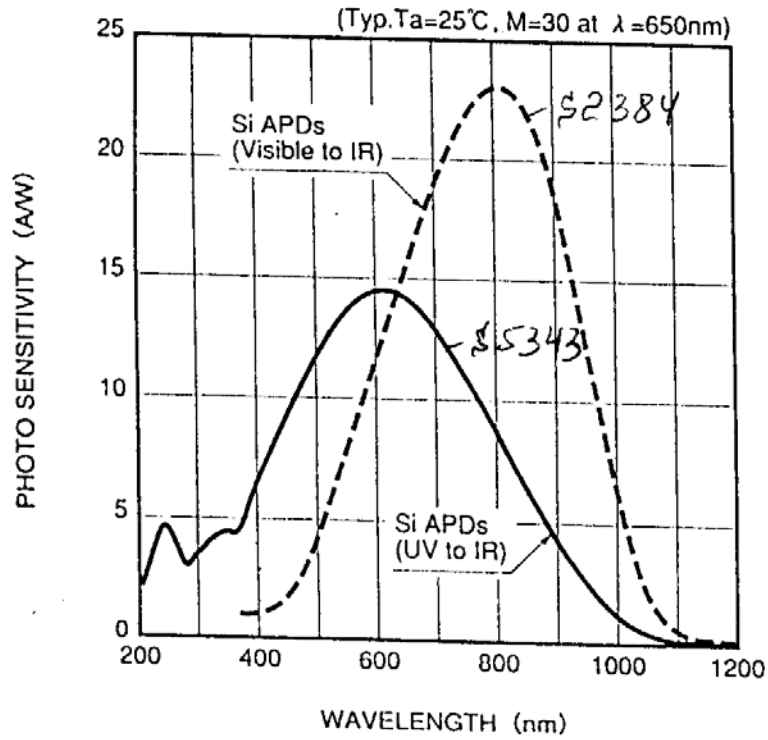


Figure 2: Spectral sensitivity of a) APDs investigated and b) of the PM XP2020 [10]

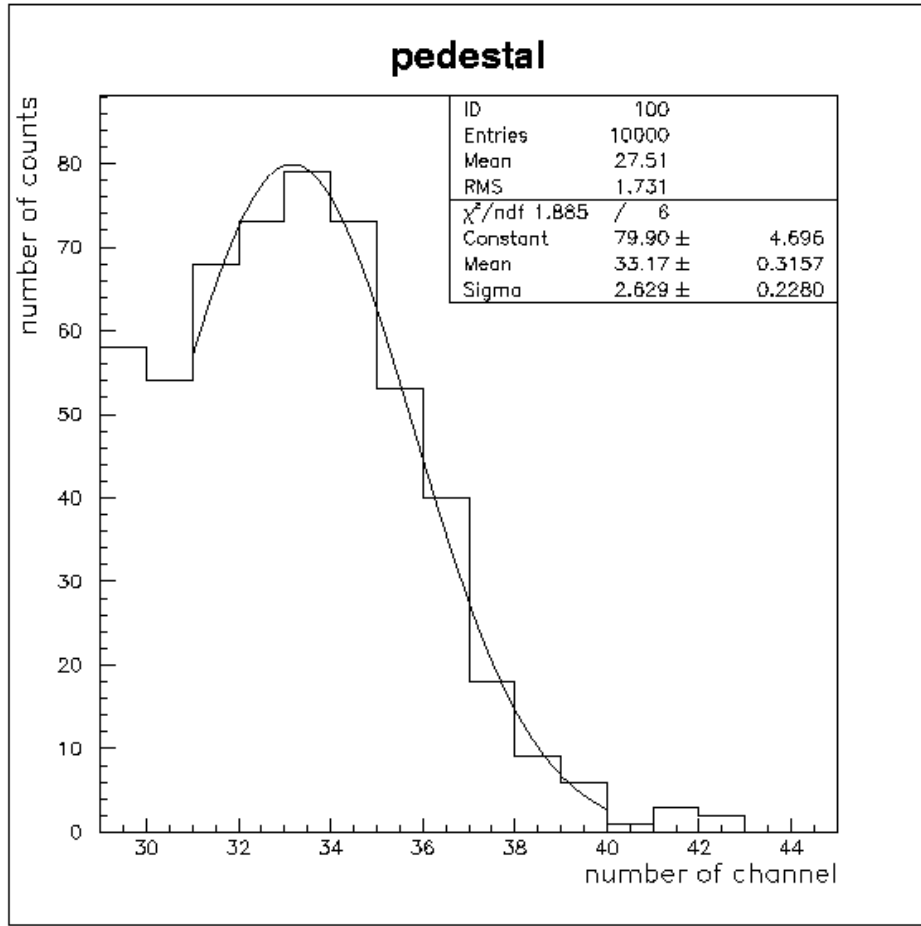


Figure 3: One-photoelectron spectrum of LED light fitted by a Gaussian

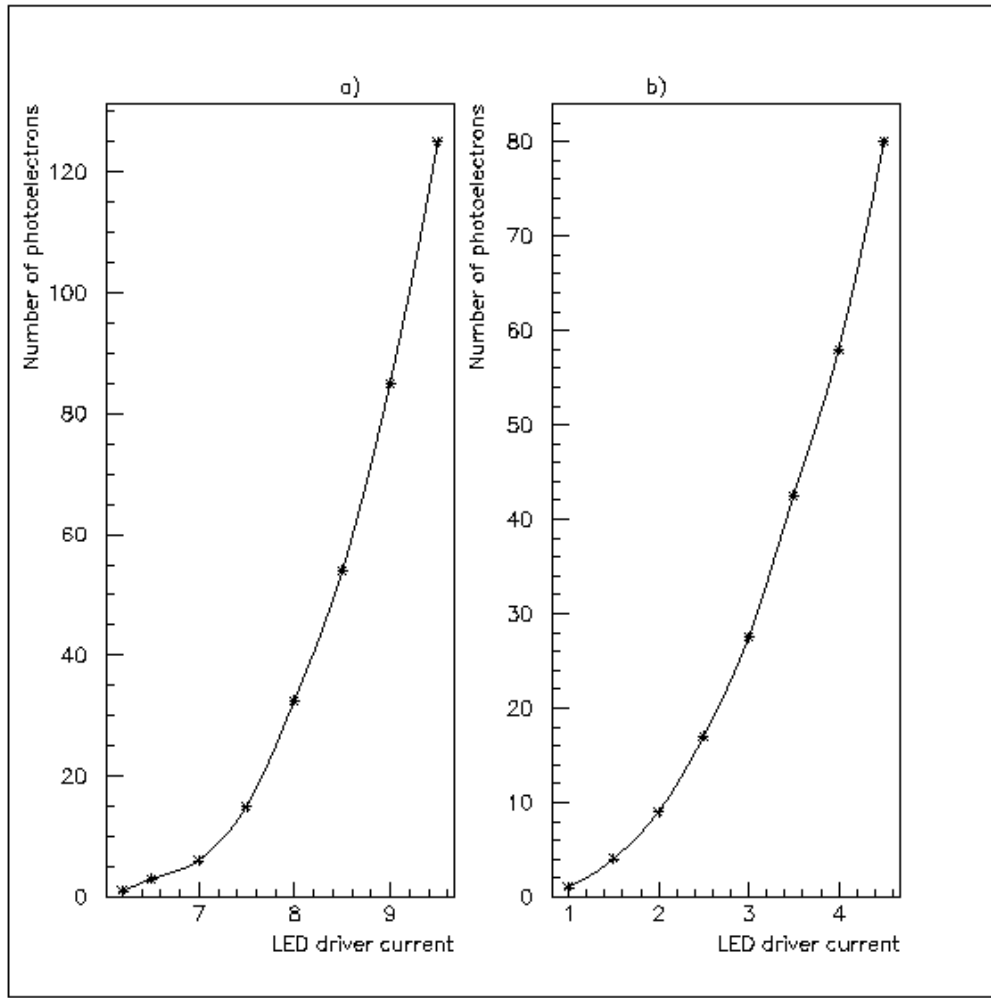


Figure 4: Calibration of LEDs by PM XP2020: a) blue LED, b) green LED, Number of photoelectrons vs. driver current in arbitrary units

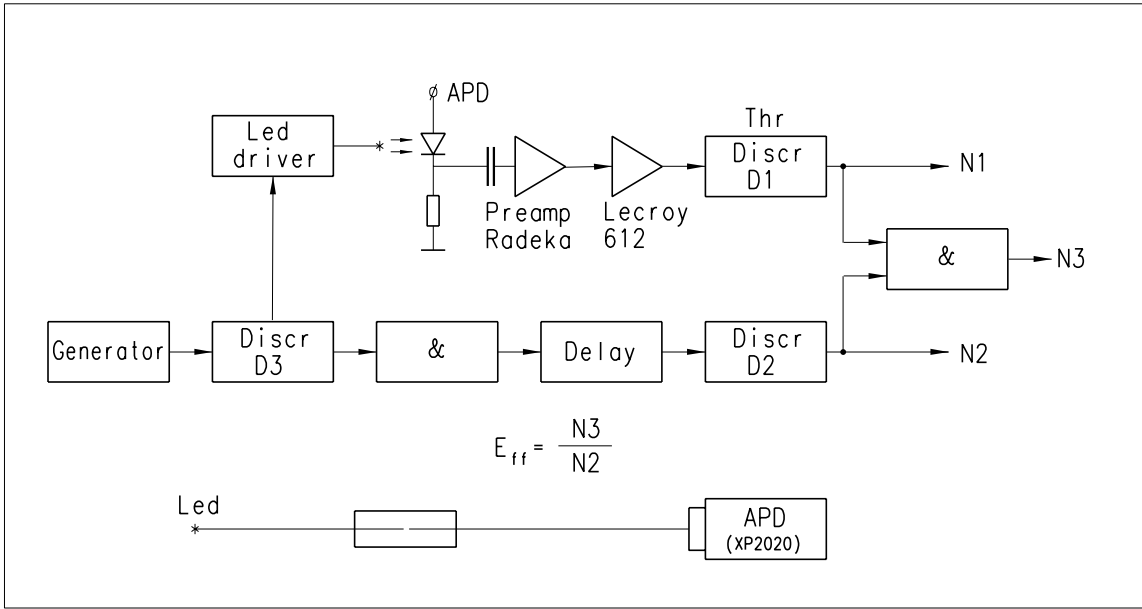


Figure 5: Experimental setup for the measurement of the sensitivity characteristics in the avalanche mode using LEDs

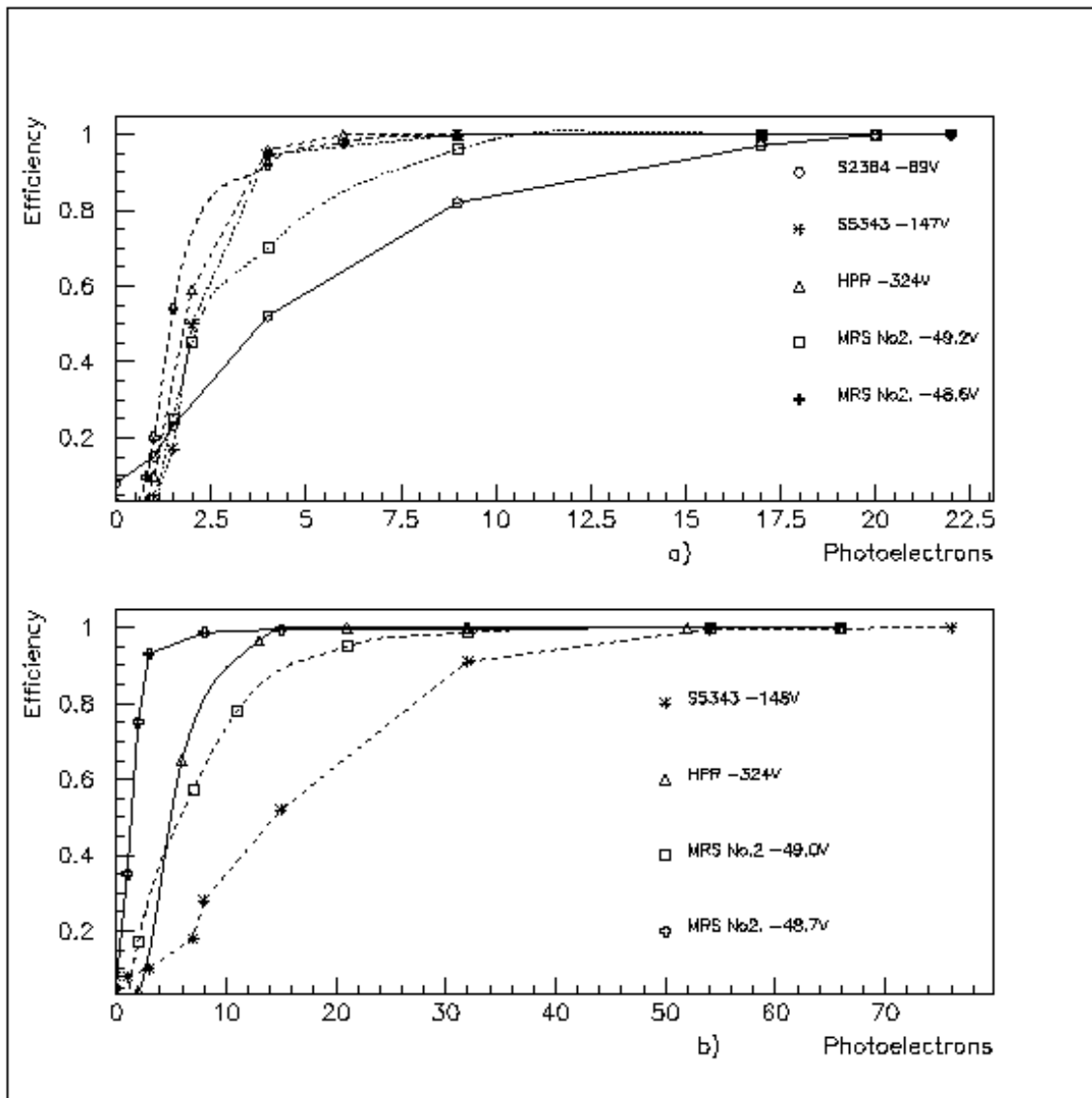


Figure 6: Efficiency vs. light amplitude measured in photoelectron equivalents of the PM XP2020 a) for green LEDs and b) for blue LEDs

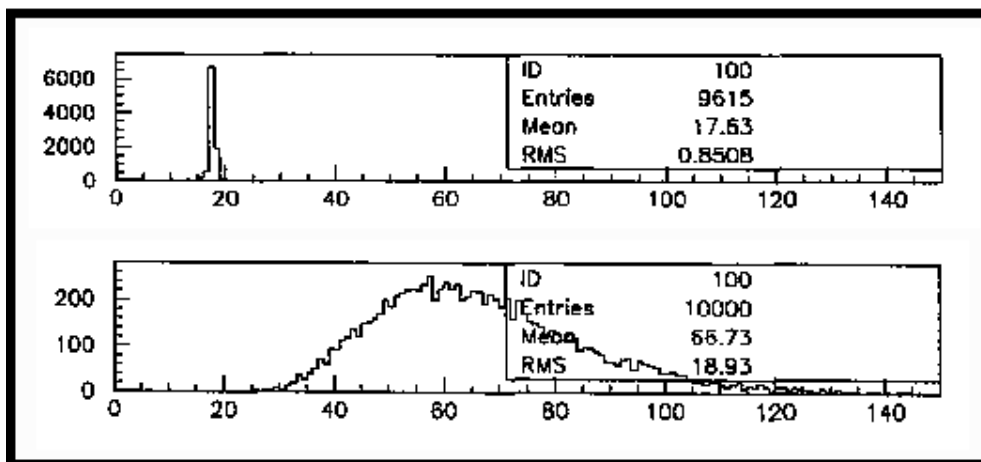


Figure 7: Pedestal and amplitude spectra of an APD type S5343 with an incident light level of 100 photons

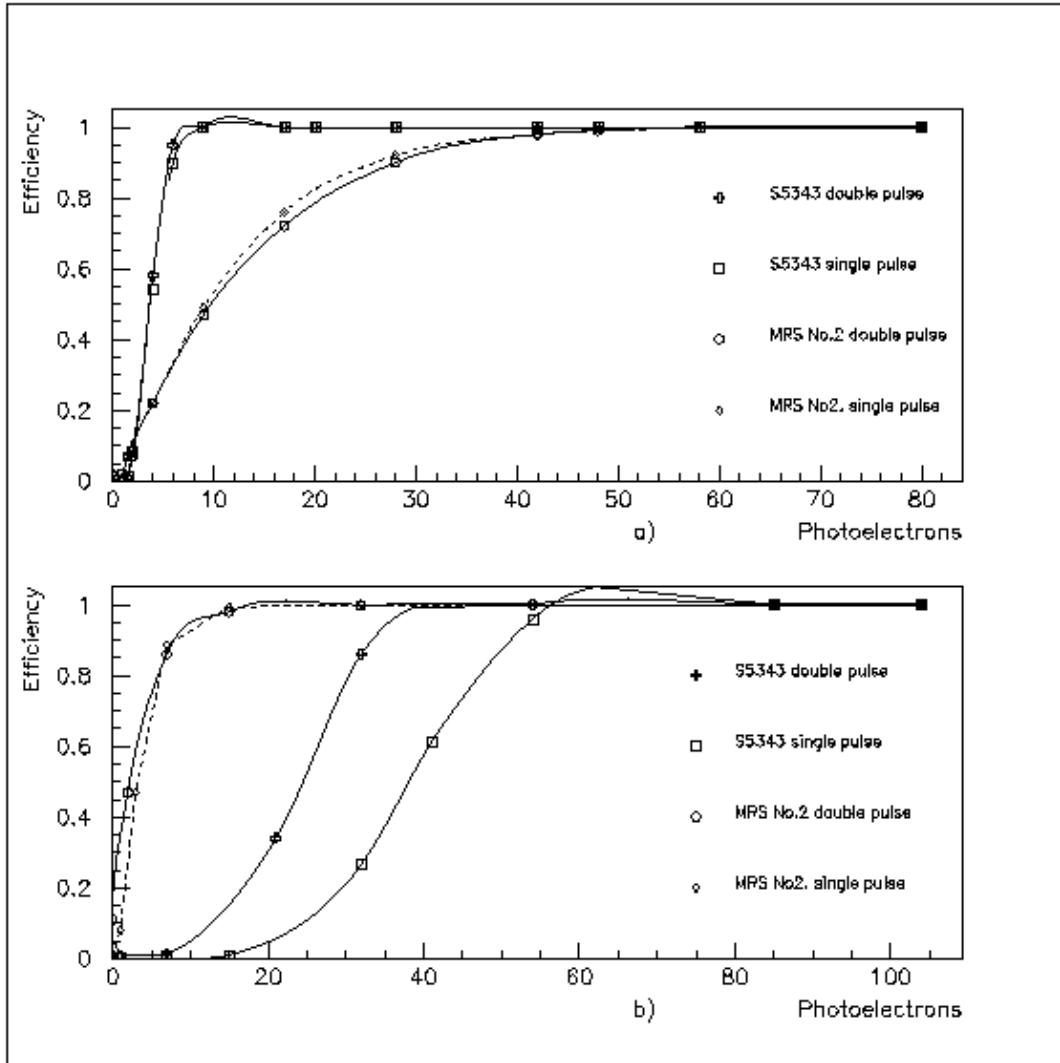


Figure 8: Efficiency of the registration of double pulses of APDs vs. light amplitude measured in photoelectron equivalent of the PM XP2020 for a) green LED and b) blue LED, LED current in arbitrary units

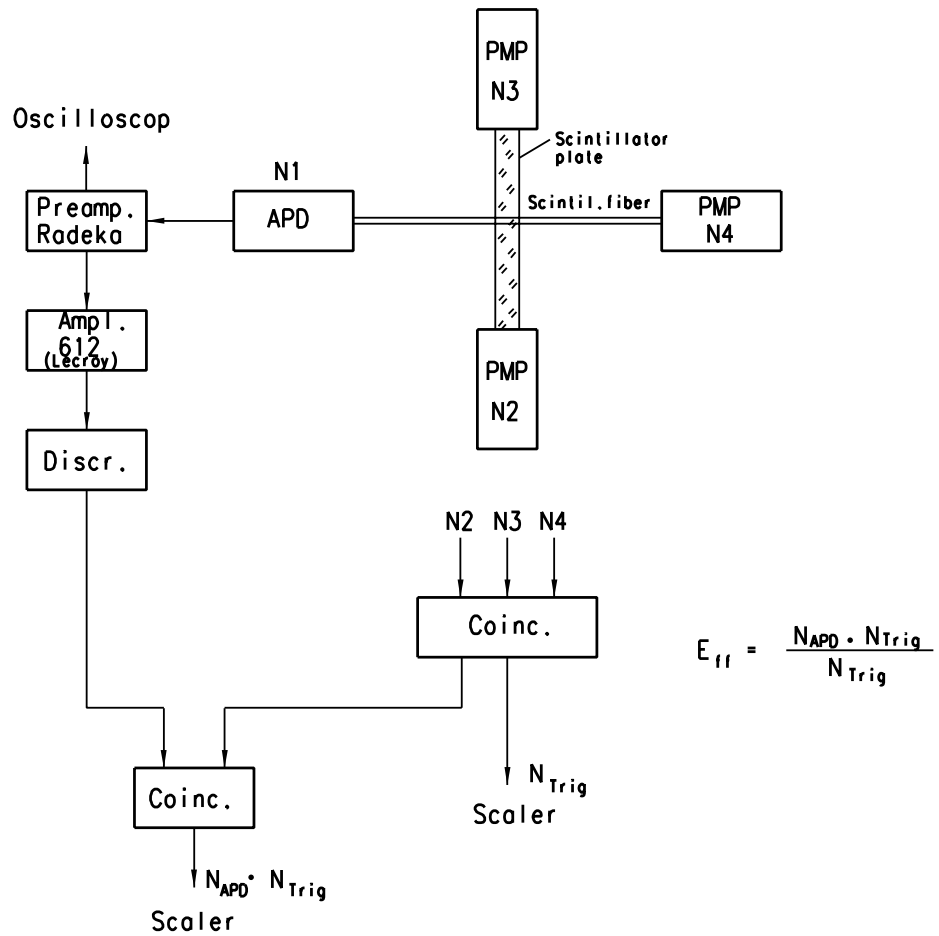


Figure 9: Experimental setup for investigations using scintillating fibers

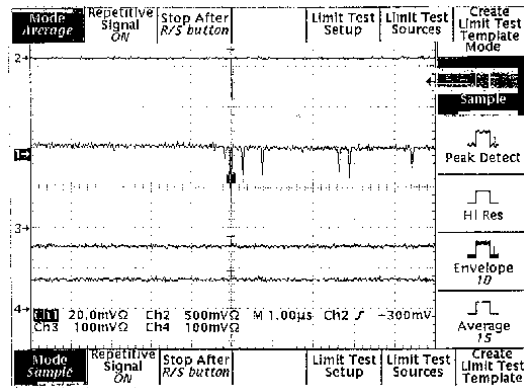
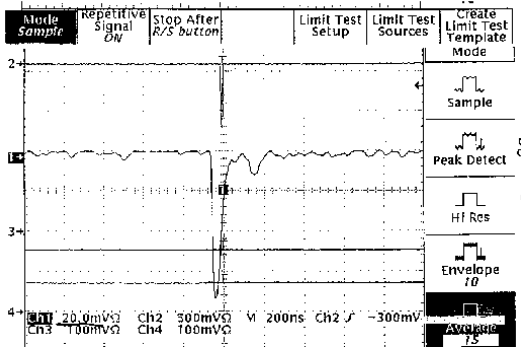
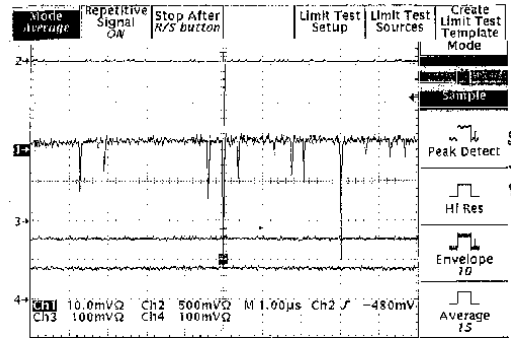
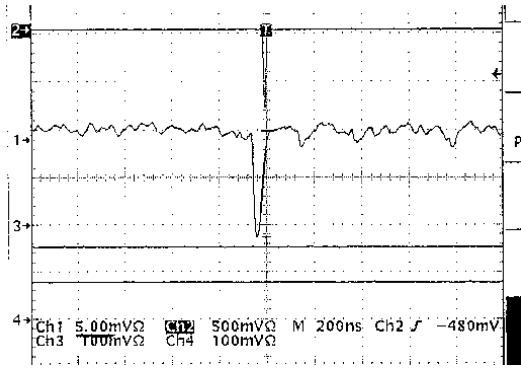


Figure 10: Signals of the APD MRS No.2(48) ($U = -48.8$ V) excited by scintillating fibers of 0.5 mm diameter measured by oscilloscope (amplifier of Radeka type), a) Averaged signal, $+20^{\circ}\text{C}$, b) Signal in sampling mode $+20^{\circ}\text{C}$, c) averaged signal, 10°C , d) Signal in sampling mode, 10°C